JOURNAL OF DENTISTRY 42 (2014) 1078–1095

Available online at www.sciencedirect.com

ScienceDirect

journal homepage: www.intl.elsevierhealth.com/journals/jden

One-pot synthesis of antibacterial monomers with dual biocidal modes

Wei Zhang [a,1], Xiao-juan Luo [a,1], Li-na Niu [b,1], Si-ying Liu [c], Wan-chun Zhu [d], Jeevanie Epasinghe [e], Liang Chen [f], Guo-hua Li [g], Cui Huang [c], Jing Mao [a,**], David H. Pashley [h], Franklin R. Tay [h,*]

[a] Department of Stomatology, Tongji Hospital, Huazhong University of Science and Technology, Wuhan, China
[b] State Key Laboratory of Military Stomatology, Department of Prosthodontics, School of Stomatology, The Fourth Military Medical University, Xi'an, China
[c] Hospital of Stomatology, Wuhan University, Wuhan, China
[d] Department of Stomatology, North Sichuan Medical College, Nanchong, China
[e] Prince Philip Dental Hospital, The University of Hong Kong, Hong Kong Special Administrative Region
[f] Research and Development, Bisco Inc., Schaumburg, IL, USA
[g] Department of Stomatology, Fuzhou Dongfang Hospital, Fuzhou, China
[h] College of Dental Medicine, Georgia Reagents University, Augusta, GA, USA

ARTICLE INFO

Article history:
Received 14 May 2014
Received in revised form
27 May 2014
Accepted 3 June 2014

Keywords:
Antibacterial
Biofilm
Dual biocidal modes
Interface
Universal adhesive

ABSTRACT

Objectives: The present study reported a method for preparing a blend of antibacterial quaternary ammonium silanes and quaternary ammonium methacryloxy silane (QAMS) based on the sol–gel reaction between dimethyldiethoxy silane and two trialkoxysilanes, one with an antibacterial quaternary ammonium functionality and the other with a methacryloxy functionality.

Methods: Reaction products of the sol–gel reaction were characterised by direct infusion mass spectrometry, FTIR and proton, carbon and silicon NMR. This blend of monomers was incorporated into an experimental universal adhesive for evaluation of antimicrobial activity against *Streptococcus mutans* biofilms, microtensile bond strength and cytotoxicty. Retention of quaternary ammonium species on polymerised adhesive, leaching of these species from the adhesive and the ability of resin–dentine interfaces to inhibit *S. mutans* biofilms were evaluated over a 3-month water-ageing period.

Results: The antibacterial adhesive version killed bacteria in *S. mutans* biofilms not only through the release of non-copolymerisable quaternary ammonium silane species (release-killing), but also via immobilised quaternary ammonium methacryloxy silane that are copolymerised with adhesive resin comonomers (contact-killing). Contact-killing was retained after water-ageing. The QAMS-containing universal adhesive has similar tensile bond strength as the control and two commercially available universal adhesives, when it was used for bonding to dentine in the etch-and-rinse mode and self-etching mode. Incorporation of the antimicrobial quaternary ammonium species blend did not adversely affect the cytotoxicity of the universal adhesive formulation.

Conclusions: Instead of using quaternary ammonium dimethacrylates and nanosilver, an alternative bimodal antimicrobial strategy for formulating antimicrobial universal dentine adhesives is achieved using the one-pot sol–gel synthesis scheme.

Clinical Significance: The QAMS containing universal dentine adhesives with dual antimicrobial activity is a promising material aimed at preventing second caries and prolonging the longevity of resin composite restorations.

© 2014 Elsevier Ltd. All rights reserved.

* *Corresponding author at*: Department of Endodontics, College of Dental Medicine, Georgia Reagents University, Augusta, GA, USA. Tel.: +1 706 721 2033; fax: +1 706 721 6252.
** *Corresponding author*.
E-mail addresses: maojing@hust.edu.cn (J. Mao), ftay@gru.edu (F.R. Tay).
[1] These authors contributed equally to this work.
http://dx.doi.org/10.1016/j.jdent.2014.06.001
0300-5712/© 2014 Elsevier Ltd. All rights reserved.

1. Introduction

Antimicrobial polymer coatings represent a class of biocides that has become increasingly important as alternatives to topically applied biocidal solutions and aerosols.[1] These antibacterial polymers may be broadly classified into biocide-releasing polymers and contact-killing biocidal polymers.[2] Although impregnation of releasable biocides such as silver nanoparticles or antibiotics into polymers represents a highly effective strategy for rapid killing of microbes, the gradually decreasing level of the released biocide may result in sub-inhibitory biocidal concentrations in the vicinity of the coatings, with the potential for developing antimicrobial resistance. To circumvent these problems, polymers have been designed with antimicrobial functional groups that are covalently immobilised on the material surface.[3] A conceivable advantage of this alternative strategy is that antimicrobial efficiency is less likely to deteriorate by the wear of the polymer coating. A potential disadvantage of the alternative strategy, however, is that unless the killed microbes are periodically removed, their accumulation over the coating surface will reduce the antimicrobial efficiency of the coating over time. Attempts to incorporate the two antibacterial strategies into a single system have recently been reported by various authors.[4–6] These dual-functional polymeric coatings demonstrated very high initial antimicrobial effectiveness due to the leaching of the non-polymerisable biocidal agent, followed by significant sustained antimicrobial activity contributed by the immobilised contact-killing biocidal polymer after exhaustion of the leachable biocidal agent.

One of the earliest examples of non-leaching organosilicon quaternary ammonium compounds capable of killing microorganisms on contact was reported in the early 1970s. Research scientists from Dow Corning Corporation found that surface bound 3-(trimethoxysilyl)-propyldimethylalkyl ammonium chloride possessed the most effective bactericidal and fungicidal properties when its quaternary ammonium alkyl chain consisted of 18 carbons.[7] After extensive toxicological testing, Dow Corning applied to the U.S. Environmental Protection Agency for industrial registration of 3-(trimethoxysilyl)-propyldimethyloctadecyl ammonium chloride (SiQAC).[8] The free SiQAC (*aka* Dow Corning 5700) won an IR-100 award for one of the best products to be commercialised in 1977. Being an antimicrobial quaternary ammonium silane (QAS), SIQAC had since been applied as coatings on garment fabrics and the surface of medical prostheses.[9–13] It is generally believed that SIQAC and other surface-immobilised quaternary ammonium or phosphonium compounds kill bacteria by contact as a result of both the penetration and interruption of the bacterial membrane by their long alkyl chains, and the increased osmotic pressure between the bacterial cytoplasm and the low-ionic strength surroundings.[1]

Because SiQAC does not possess functional groups that enable it to copolymerise with other organofunctional monomers, a generic coupling scheme has recently been developed using the sol–gel synthesis route. This scheme uses a tetralkoxysilane as the anchoring unit for coupling the SIQAC trialkoxysilane to another trisialkoxysilane containing the designated organic functionality.[14] The sol–gel synthesis route is a highly effective method for the synthesis of crystalline and amorphous silica and organosilicates under mild conditions.[15] By introducing organic functionalities into the inorganic silica/silicate matrices, the properties of the sol–gel derived materials may be tailored at the molecular level according to different requirements.[16,17] An example of this facile synthesis scheme is the use of tetraethoxysilane (TEOS) for coupling SIQAC to 3-(trimethoxysilyl)propyl methacrylate (3-MPTS).[18] An antimicrobial quaternary ammonium methacryloxy silane (QAMS) molecule is formed, which can be dissolved in low concentration in methyl methacrylate to produce a methacrylate resin comonomer blend. When this comonomer blend was mixed with poly(methyl) methacrylate powder, an antimicrobial orthodontic acrylic was produced that has retained in vitro contact-killing effects against bacteria commonly encountered in dental caries, as well as fungus present in oral candidiasis, for up to 3 months.[19]

In sol–gel synthesis of silica and silicate, matrix-forming precursors such as TEOS and tetramethoxysilane (TMOS) are preferred as anchoring units because they have four functional groups undergoing hydrolysis and condensation to create three-dimensional silica/silicate networks. Nevertheless, the use of tetrafunctional alkoxysilane as the precursor renders the so-formed QAMS molecule insoluble in most dimethacrylates that are employed in the formulation of dental resin composites and adhesives. Although the TEOS-derived QAMS molecule is soluble in methyl methacrylate and ethanol, methyl methacrylate is a potent contact allergen and its application as a comonomer is dentine adhesives is restricted.[20] The limited solubility of the TEOS-derived QAMS molecule in solvents such as methanol, ethanol or acetone also poses problems in dentine bonding. Evaporation of the non-methacrylate solvent can result in phase separation of the dimethacrylate components, thereby jeopardising the bond strength of the adhesive comonomer blend to dentine in the presence of water originating from the dentinal tubules.[21–23] In the formulation of dentine adhesives, it is customary to employ resin monomers that are soluble in 2-hydroxyethyl methacrylate (HEMA), because the latter is miscible with water and most dimethacrylate monomers; comonomers which are dissolved in HEMA do not undergo phase separation following removal of water during the bonding procedure.[24]

To circumvent the problem of limited solubility of TEOS-derived QAMS in HEMA, the authors have invented a new sol–gel synthesis method for preparing antibacterial QAMS, by replacing the tetrafunctional TEOS anchoring unit with a difunctional anchoring unit, dimethyldiethoxysilane (DMDES). Difunctional alkoxides such as DMDES cannot act as network formers due to insufficient functionalities to form three-dimensional networks.[25] The presence of non-hydrolysable organic groups (i.e. methyl instead of ethoxy) in the synthesis mixture reduces the cross-linking ability of the silicate network.[26] This tendency to form linear chains may also be used to provide some flexibility to the polymer matrix network[27], when the resultant DMDES-derived QAMS monomer is copolymerised with other dimethacrylates in dentine adhesive formulations. Because one-pot sol–gel synthesis involving multiple alkoxysilanes usually generates a series of

molecules with different molecular masses instead of a single molecule, the DEDMS-derived QAMS produced by the reaction of the dialkoxysilane with two trialkoxysilanes under alkaline condition was first characterised in the present study. Universal dentine adhesives, which are capable of bonding to enamel and dentine in the etch-and-rinse or the self-etching mode, represent the latest generation of dentine adhesives that are well-received by clinicians because of their multimode bonding capability, simplicity and user-friendliness.[28–30] Thus, the one-pot synthesised DMDES-derived QAMS mixture was dissolved in HEMA and incorporated into a hydrophilic dimethacrylate comonomer blend to create an experimental, antibacterial universal dentine adhesive. The antibacterial property of the polymerised universal adhesive was examined using *Streptococcus mutans* biofilms which are commonly found in initial dental caries. The ability of this antibacterial universal adhesive for bonding to crown dentine was investigated, with further examination of the antibacterial potential of the resin–dentine interface after 3 months of water-ageing. For the antibacterial universal adhesive, the hypotheses tested were: (i) incorporation of DMDES-derived QAMS into an experimental universal adhesive does not compromise the bond strength of the adhesive to dentine when it is used in the etch-and-rinse mode or the self-etching mode; and (ii) inclusion of a blend of quaternary ammonium species with and without methacryloxy functional groups, created by one-pot sol–gel processing within the experimental universal adhesive, results in both initial release-killing and retained contact-killing activity in the resin–dentine interface against *S. mutans* biofilms after 3 months of water-ageing.

2. Materials and methods

2.1. Synthesis of DMDES-derived QAMS

Dimethyldiethoxylsilane (DMDES), 3-(trimethoxysilyl)-propyldimethyloctadecyl ammonium chloride (SiQAC) and 3-(trimethoxysilyl)propyl methacrylate (3-MPTS) were obtained from Sigma–Aldrich (St Louis, MN, USA) and used without further purification. The QAMS monomer mixture was prepared by adding DMDES, SiQAC, and 3-MPTS in a 1:1:1 molar ratio. Basic MilliQ water (pH 10, prepared using 0.01 N NaOH) was added to the QAMS mixture, using a water-to-precursor molar ratio of 4 (12 moles of water to 48 moles of reactants), as catalyst for the sol–gel reaction and to ensure optimal hydrolysis of the dialkoxysilane and trialkoxysilanes. The mixture was stirred for 6 h at ambient temperature for completion of the hydrolysis–condensation reactions, followed by vacuum-stripping for 24 h to remove the sol–gel reaction by-products (i.e. water and alcohols) from the rubbery organically modified silicate condensate.

2.2. Characterisation of DMDES-derived QAMS

2.2.1. Direct-infusion mass spectrometry (DIMS)

The water- and alcohol-depleted QAMS was dissolved in methanol at a concentration of 35% (w/v). Direct infusion mass spectrometry analysis was performed using a Finnigan LTQ mass spectrometer (Thermo Fisher Scientific, Waltham, MA, USA) with electrospray ionisation (ESI) in the positive ion mode. The conditions for direct infusion analysis were: mass-to-charge range (150–2000 *m/z*); capillary voltage (28.84 V) and ESI spray current (19 μA). The analyte solution was continuously introduced by the ESI needle to the ion source in the spray chamber which was a high voltage region. The needle was placed inside a larger capillary through which nitrogen gas was pumped to nebulise the solution. Upon nebulisation, the analyte molecules were ionised by cations, predominantly H^+ ions from the solution. The charged droplets passed across an electric field between the electrodes at a higher voltage relative to the heated capillary. The ions were electrostatically guided and drifted towards the relatively high negative voltage. In doing so, the ions entered the heated capillary and proceeded into the analyser region. Data processing involved multiple scanning of the mass range (200–1200 *m/z*) for about 3 min to obtain a mass-to-charge ratio (*m/z*) spectrum with relative signal intensity for each ion detected.

2.2.2. Attenuated total reflection-Fourier transform infrared spectroscopy (ATR-FTIR)

A Nicolet 6700 FTIR spectrophotometer (Thermo Fisher Scientific) with an ATR set-up was used for analysis. As no photoinitiator was used in the material prepared for ATR-FTIR, the overall IR spectra collected between 4000 and 400 cm^{-1} at 4 cm^{-1} were normalised and superimposed with respect to the aliphatic C≡C band of the methacryloxy groups at 1636 cm^{-1}.

2.2.3. Nuclear magnetic resonance spectroscopy (NMR)

For proton (^1H) NMR, the QAMS sample was dissolved in CD_3OD (Sigma–Aldrich) to 10% (m/v) concentration before testing. Spectra were acquired from 15 to −2 ppm with a 45° pulse angle of 6 μs using a Varian Mercury NMR spectrometer (Varian Inc., Palo Alto, CA, USA). All chemical shifts were referenced manually using the resonance frequency of CD_3OD. For carbon (^{13}C) NMR, the QAMS sample was similarly dissolved in CD_3OD to 10% (m/v) concentration before testing. Spectra were acquired from 230 to −20 ppm with an 80–90° pulse angle of 12 μs. Composite pulse decoupling was used to remove proton coupling. For silicon (^{29}Si) NMR, the water- and alcohol-depleted QAMS was examined in the solid state using ^{29}Si Cross Polarisation-Magic Angle Spinning (CP-MAS) NMR. Analysis was performed with a 270 MHz spectrometer (JEOL, Tokyo, Japan) equipped with a 7 mm MAS probe. Spectra were acquired using a MAS frequency of 4 kHz, with a 45° pulse angle of 5 μs. Chemical shifts were referenced to tetramethylsilane at ±0.3 ppm.

2.3. Preparation of QAMS-containing universal dentine adhesive

A universal adhesive was prepared containing 20 wt% HEMA, and with the other 80 wt% consisting of proprietary amounts of 10-methacryloyloxydecyl dihydrogen phosphate (10-MDP), bisphenol A diglycidyl ether methacrylate (bis-GMA), ethanol, water, camphorquinone and a proprietary tertiary amine (courtesy of Bisco Inc., Schamburg, IL, USA). This was employed as the non-antibacterial, ''control version'' of the universal adhesive (Lot 728-95a).

For preparing the antibacterial universal adhesive, 35 wt% of the vacuum-stripped DMDES-derived QAMS solid was first dissolved in HEMA to produce a HEMA-QAMS solution. Six trial versions of the universal adhesive were initially prepared by replacing the 20 wt% of HEMA in the ''control version'' with (a) 14 wt% HEMA and 6 wt% HEMA-QAMS, (b) 12 wt% HEMA and 8 wt% HEMA-QAMS; (c) 10 wt% HEMA and 10 wt% HEMA-QAMS; (d) 8 wt% HEMA and 12 wt% HEMA-QAMS; (e) 6 wt% HEMA and 14 wt% HEMA-QAMS; and (f) 20 wt% HEMA-QAMS. The other 80 wt% of the composition in these trial versions was the same as the ''control version''. These 6 trial formulations were used for bonding to dentine in the etch-and-rinse mode and the bonded specimens were subjected to microtensile bond testing (described below). Because there were no differences in microtensile bond strength among the six versions (data not shown), the version with the highest concentration of HEMA-QAMS (i.e. 20 wt%) was chosen as the ''antibacterial experimental version'' of the universal adhesive (Lot 728-95b). The amount of DMDES-derived QAMS present in this ''antibacterial experimental version'' was 7 wt%.

2.4. *Adhesive-coated dentine disks for evaluation of antimicrobial activity*

Caries-free extracted human wisdom teeth were obtained with the patients' consent under a protocol that was approved by the Human Assurance Committee of the Georgia Regents University. These teeth were stored in 0.9% NaCl containing 0.02% sodium azide to prevent bacteria growth. For each tooth, mid-coronal dentine along the occlusal plane was exposed by removing the occlusal enamel with a diamond blade (Isomet, Buehler Ltd., Lake Bluff, IL, USA) under copious water cooling. The exposed dentine was ground with 600-grit silicon carbide paper for 30 s under water cooling prior to bonding.

For growing of biofilms, the dentine disks were bonded in the etch-and-rinse mode, using either the control version or the experimental version of the universal adhesive ($N = 10$). Each dentine surface was etched with 32% phosphoric acid gel (Uni-Etch, Bisco, Inc.) for 15 s and rinsed with water for 20 s. Two coats of the respective control or experimental universal adhesive were applied to the visibly moist acid-etched dentine, with 15 s of adhesive agitation for each coat. The adhesive was air-dried for 5 s, and light-activated for 10 s using a light-curing unit (XL 3000, 3M ESPE, St. Paul, MN, USA).

Prior to the use of these adhesive-coated dentine disks for growing biofilms, the disks were immersed in sterile deionised water and agitated at 200 cycles per min for one min to remove unpolymerised monomers within the surface air-inhibition layer.

2.5. *Antibacterial assay*

2.5.1. *Bacterial culture and biofilm preparation*

S. mutans (ATCC 35668; American Type Culture Collection, Manassas, VA, USA) was used for the formation of single-species biofilms. The bacteria were cultured in Brain Heart Infusion (BHI) broth (Difco, Becton-Dickinson and Co., Sparks, MD, USA) supplemented with 50 mM sucrose (pH 7.3). Bacteria cells were harvested from 24-h fresh culture by centrifuging at 4000 rpm for 10 min. The cell pellet was washed three times with sterile phosphate buffered saline (PBS, 0.01 M, pH 7.3), re-suspended in 100 mL of the growth medium, and further adjusted with growth medium to a concentration of 10^7 CFU/mL.

The adhesive-coated dentine disks from the control group and the QAMS-containing experimental group ($N = 6$) were disinfected under ultraviolet light (wavelength = 200–290 nm, irradiance = 30 mW/cm^2, light-to-target distance = 60 cm) for 2 h before transferring to the specimen holder of an oral biofilm reactor. The biofilm reactor consisted of a reactor vessel and a specimen holder with 18 recessed holders for insertion of substrate disks over which bacteria biofilms could be grown.[18] The six disks from each group were affixed to the sample ports of the specimen holder, and incubated in pooled sterile saliva for 1 h at 37 °C to create a salivary pellicle on the surface. Sterile pooled saliva was obtained by collecting whole saliva from three healthy volunteers without stimulation (flow rate 0.25 mL/min; pH 7.3). The pooled saliva was centrifuged at 2000 rpm for 15 min to remove cellular debris, oral microorganisms and particles. The supernatant was mixed with dithiothreitol (Sigma–Aldrich, 2.5 mmol/L) to reduce salivary protein aggregation, and centrifuged again at 2000 rpm for 15 min at 4 °C. The supernatant was then filter-sterilised through sterile 0.22 μm disposable membrane filters (Nalge Numc International, Rochester, NY), and stored at 20 °C until use.

The specimen holder with the pellicle-containing, adhesive-coated dentine disks from the two groups was then transferred to the reactor vessel which was subsequently filled with *S. mutans* cell suspension (10^7 CFU/mL). The assembly was first incubated for 90 min at 37 °C in an orbital shaker incubator at 50 rpm, to develop the adhesion phase of the respective biofilm. Following the adhesion phase, the specimen holder was removed, rinsed carefully with 100 mL of sterile PBS (0.01 M, pH 7.3), and transferred aseptically to a new, sterile reactor vessel, which held the disks on a fixed stage in 200 mL of the growth medium. The assembly was placed over an orbital incubator (37 °C; 50 rpm), and connected to several vessels (nutrient, sucrose solution, and waste) and to an infusion pump, to complete the in vitro artificial mouth system. A desired flow rate was established before allowing biofilm formation to proceed for 24 h. The flow rate was adjusted according to the chemostat mode at a dilution rate of 0.10 h^{-1}. *S. mutans* biofilms were grown under anaerobic conditions (5% carbon dioxide, 10% hydrogen and 85% nitrogen). At the end of the 24-h growth period, the specimen holder with the adhesive-coated dentine discs was aseptically removed and immersed in 100 mL of sterile PBS to remove non-adherent bacteria cells. The adhesive-coated dentine disks with adherent biofilms were then retrieved for further investigation.

2.5.2. *Confocal laser scanning microscopy (CLSM)*

Biofilms grown on top of the adhesive-coated dentine disks from the control and experimental universal adhesive groups were stained with a LIVE/DEAD® BacLight™ Bacterial Viability Kit (Molecular Probes, Eugene, OR, USA). Live bacteria were stained with SYTO-9 to produce green fluorescence, and bacteria with compromised membranes were stained with

propidium iodide (PI) to produce red fluorescence. SYTO-9 and PI were activated at wavelengths of 488 and 568 nm respectively, and imaged using a CLSM (LSM 510 META, Zeiss, Jena, Germany) at 40× magnification. For each of the six adhesive-coated dentine disks in each group, two image stacks (Z-stack) were obtained at locations that were characteristic of each biofilm on that disc. Images (field size: 212 μm × 212 μm) were acquired at a Z-step of 2 μm (i.e. distance between two adjacent images of a stack), beginning from the bottom of the biofilm that was in contact with the adhesive surface, to the top of the biofilm. Images from each stack were analysed using image analysis software (BioImageL v2.1; Faculty of Odontology, Malmö University, Malmö, Sweden). The biovolume of interest, representing the first 24 μm of each Z-stack (i.e. 1st–13th images), was analysed for the percentage distribution of live and dead bacteria. A constant biofilm thickness model for CLSM analysis was employed to eliminate the effect of varied biofilm thickness.

2.5.3. *Colony forming unit (CFU) counts*

After biofilm formation, two of the six adhesive-coated dentine disks from each group were placed in a microtube containing 1 mL of PBS and vortexed for 2 min to detach the biofilm. Ten-fold serial dilutions were generated in sterile PBS (0.01 mM, pH 7.3), and each dilution was plated (50 μL aliquots) onto brain heart infusion agar plates. The plates were incubated at 37 °C for 48 h in an anaerobic chamber. After incubation, the CFUs of *S. mutans* per adhesive-coated disc were calculated manually. Five replicates were performed for each adhesive-coated dentine disc in each group ($N = 10$). Statistical comparison of the CFU data derived from the two groups was performed using Student's *t*-test at $\alpha = 0.05$, following logarithmic transformation to render the data suitable for the application of parametric statistical methods.

2.5.4. *XTT assay*

The other four biofilm-containing disks from each group were transferred into separate microtubes containing 4 mL of sterile PBS (0.01 mM, pH 7.3), avoiding disturbances to the biofilms. Fifty microlitres of 1 mg/mL solution of 2,3-bis-(2-methoxy-4-nitro-5-sulfophenyl)-2H-tetrazolium-5-carboxanilide (XTT; Sigma–Aldrich) and 4 μL of 1 mM menadione (Sigma–Aldrich) were then added to each microtube. The solutions were mixed gently, covered with aluminium foil and incubated for 5 h at 37 °C. After incubation, the solution was transferred to a new microtube and centrifuged at 4000 rpm for 10 min at 4 °C. The supernatant was placed in a 96-well plate and read at 492 nm using a spectrophotometer (Victor, R & D systems, Minnesota, USA). Three readings were taken for each adhesive-coated dentine disc from each group ($N = 12$). Statistical comparison of the CFU data derived from the two groups was performed using Student's *t*-test at $\alpha = 0.05$.

2.6. *Transmission electron microscopy (TEM)*

The ultrastructure of the resin-dentine interface of dentine specimens bonded with the control or the experimental version of the universal adhesive was characterised using TEM. For each adhesive version, bonding was performed in both the etch-and-rinse mode and the self-etching mode ($N = 2$). Bonding procedures described in the previous section were used for dentine bonding in the etch-and-rinse mode. For bonding in the self-etching mode, the control or the experimental universal adhesive was used to prime the dentine surface twice without rinsing, with 15 s of adhesive agitation for each adhesive coat. The adhesive was air-dried for 5 s, and light-activated for 10 s.

A 2-mm thick strip was sectioned from the centre portion of each adhesive-coated dentine disc. Each strip, containing the adhesive-dentine interface, was fixed in modified Karnovsky's fixative (2.5% glutaraldehyde and 2% formaldehyde in 0.1 M cacodylate buffer) for 4 h, rinsed in cacodylate buffer, post-fixed in 1% osmium tetroxide for 1 h, dehydrated in an ascending ethanol series, substituted with propylene oxide and embedded in epoxy resin, according to the TEM embedding protocol previously reported by Tay et al.[31] Non-demineralized, 90–100 nm thick sections were prepared and examined unstained using a transmission electron microscope (JEM-1230, Tokyo, Japan) at 110 kV.

2.7. *Microtensile bond strength evaluation*

The control universal adhesive (without DMDES-derived QAMS) and the experimental universal adhesive (containing 7% DMDES-derived QAMS) were used for bonding to mid-coronal dentine in the etch-and-rinse mode or the self-etching mode as previously described. For comparison, two commercially available universal adhesives, All-Bond Universal (Bisco, Inc.) and Scotchbond Universal Adhesive (3M ESPE) were used in their respective etch-and-rinse mode and self-etching mode for bonding to mid-coronal dentine, according to the instructions recommended by the respective manufacturer. Six teeth were used for each adhesive and each bonding mode ($N = 6$). Following adhesive application and light-curing, four 1-mm increments of a resin composite (AP-X; Kuraray Co. Ltd., Tokyo, Japan) were incrementally placed over the cured adhesive and light-activated individually for 40 s. The bonded teeth were stored in 100% humidity at 37 °C for 24 h. The resin-bonded specimens were vertically sectioned into 0.9 mm thick slabs. The centre slab was saved for evaluation of antibacterial activity after water-ageing. The two adjacent slabs were sectioned into 0.9 mm × 0.9 mm beams; the two longest beams from each slab were used for microtensile bond strength testing. Thus, for each adhesive and each bonding mode, twenty-four beams (two beams per slab × two slabs per tooth × six teeth) were used for microtensile testing ($N = 24$). Each beam was stressed to failure under a load applied with a universal testing machine (Vitrodyne V1000, Chatillon, Greensboro, NC, USA) at a crosshead speed of 1 mm/min. Beams that failed during specimen preparation were recorded as null bond strength. Statistical comparison was performed individually for each bonding mode, with dentine beam used as the statistical unit. Because the data sets were normally distributed and exhibited equal variance, statistical comparisons for each bonding mode were performed using one-factor ANOVA and Tukey multiple comparison test at $\alpha = 0.05$.

2.8. Remnant and leachable quaternary ammonium species after water-ageing

2.8.1. Sodium fluorescein binding assay

The amount of quaternary ammonium species retained on the surface of the polymerised experimental universal adhesive (i.e. the one containing 7 wt% DMDES-derived QAMS) after a 12-week period of water-ageing was assessed using the fluorescein staining method.[32] This method was based on the ability of a single fluorescein molecule to bind to the N^+ charge of a quaternary ammonium molecule. Adhesive disks (10 mm diameter × 2 mm thick) containing 7 wt% DMDES-derived QAMs were prepared by evaporating the solvent from the experimental universal adhesive prior to light-curing ($N = 8$). Eight examinations were conducted during the 12-week water-ageing period: baseline, 1st, 2nd, 4th, 6th, 8th, 10th and 12th week. Except for the baseline, each disc was immersed in 2 mL of sterile deionised water in a separate scintillation vial at 37 °C under continuously shaking. At different time periods, each disc was retrieved from the ageing solution and placed into an individual vial containing 2 mL of a 10 mg/mL stock solution of fluorescein sodium salt (Sigma–Aldrich). Specimens were left to stand in the dark at room temperature for 10 min. Unbound fluorescein was removed by rinsing the specimens with deionised water for five times. Bound fluorescein from the QAMS-containing adhesive disks was extracted by ultrasonicating each specimen in a vial containing 1.8 mL of a 0.1 wt% cetyltrimethylammonium chloride stock solution (Sigma–Aldrich) for 20 min. An additional 0.2 mL of 100 mM of PBS (pH 8.0) was added to each vial. An absorbance spectrum of the bound fluorescein was obtained using a UV–vis spectrophotometer (160A UV-Vis spectrometer, Shimadzu, Kyoto, Japan) at 501 nm. The extinction coefficient of fluorescein in the solution was taken to be 77 $mM^{-1}\,cm^{-1}$. The number of nanomoles of fluorescein in the 2 mL solution was calculated from a calibration graph relating fluorescein concentration and absorbance, and then divided by the surface area of the specimen to generate a specific N^+ charge density value (nM/cm^2).

2.8.2. Bromophenol blue assay

Because the fluorescein binding assay did not account for the amount of QAMS released into solution as an unbound component, the amount of leached QAMS in the aged solution was determined using the bromophenol blue assay.[33] Bromophenol blue is a dye which forms a complex with quaternary ammonium compounds, and results in a shift of λ_{max} from 593 to 603 nm due to complex formation. Additional adhesive disks (10.0 mm diameter × 2.0 mm thick) containing 7 wt% DMDES-derived QAMs were prepared in the manner reported in the previous section ($N = 8$). Seven periods were examined: 1st, 2nd, 4th, 6th, 8th, 10th and 12th week. The disks were first stored in 2 mL of sterile deionised water in individual scintillation vials at 37 °C. After retrieving the eluent containing the leached QAMS at each time period, the disks were placed in fresh deionised water for continued ageing until the next collection period. For each time period, a 0.5 mL aliquot of the eluent was mixed with 1.5 mL of bromophenol blue solution (0.001 wt%; buffered with sodium carbonate to pH 7.0 to avoid absorption changes owing to pH fluctuations), and agitated gently for 10 min. Absorbance of the mixture was recorded using the UV–vis spectrophotometer at 603 nm. The molar concentrations of N^+ leachate at different time periods were read from a standard curve which was established from the absorption values of known concentrations of SiQAC (from 0 to 1.451 mM).

2.9. Retained antibacterial activity after 3 months of water ageing

The centre composite-adhesive-dentine slabs (saved from the microtensile testing experiment) in the experimental universal adhesive group were aged in sterile deionised water at 37 °C for 3 months. Specimens bonded using the etch-and-rinse mode and the self-etching mode were used for ageing. After ageing, each slab was used to grow 24-h *S. mutans* biofilm in the manner previously described. The biofilms were stained with BacLight™ stain and imaged with CLSM at 40× magnification to determine the presence of retained antibacterial activity along the resin-dentine interface after water-ageing.

2.10. Cytotoxicity evaluation

Dentine adhesive components applied to vital exposed dentine may diffuse into the pulp. This may adversely affect the survival of primary odontoblasts or odontoblast-like cells differentiated from pulpal stem cells, and the ability of these cells to produce tertiary reactionary or reparative dentine.[34] Thus, a rat odontoblast-like cell line derived from the apical papilla (MDPC-23) was employed for comparing the cytotoxicity of the control and experimental versions of the universal adhesive.[35] The two adhesives were vacuum-stripped to remove the solvent, placed in pre-sterilised Teflon moulds, covered with per-sterilised Mylar sheets, and light-cured to prepare 5-mm diameter and 2-mm thick adhesive disks that were devoid of air-inhibition layers. Untreated cells were used as the negative control. Disks of similar dimensions to the test adhesives and prepared from zinc oxide–eugenol based Intermediate Restorative Material (IRM; Dentsply Caulk, Milford, DE, USA) were assigned as the positive control. All set materials were sterilised with ultraviolet light (conditions identical to those mentioned above) for 2 h before testing. The MDPC-23 cells were plated in growth medium and incubated at 37 °C in a humidified 5% CO_2 atmosphere for 24 h until they achieved 70–80% confluency. The growth medium consisted of Dulbecco modified Eagle medium (Lonza, Wakersville, MD, USA) and 10% foetal bovine serum (Invitrogen Corp., Carlsbad, CA, USA) supplemented with 2 mmol/L L-glutamine and 100 U/mL penicillin/streptomycin.

2.10.1. Cell viability

An XTT Cell Viability Assay Kit (Biotium Inc., Hayward, CA, USA) was used to determine cell viability based on the cleavage of the yellow tetrazolium salt XTT by mitochondrial enzymes in metabolically active cells to form a soluble orange formazan product. Disks from the different groups were placed individually in transwell inserts with a 3-mm pore size (BD Falcon, Franklin Lakes, NJ, USA) to prevent direct contact of the cells. The transwell inserts were placed inside a 24-well

plate with each well covered by an equal volume (2 mL) of growth medium. The disks were exposed to the plated cells for 3 days, without further change in culture medium, before testing for mitochondrial dehydrogenase activity. Production of formazan by the metabolically active cells was quantified by measuring its absorbance at 492 nm. The absorbance of the control was adjusted to 100%, with which the relative dehydrogenase activities of the three other groups were compared ($N = 10$). Data derived from the control and experimental versions of the universal adhesive were statistically compared using Student's t-test at $\alpha = 0.05$. The IRM positive control group was excluded to increase the robustness of the statistical analysis.

2.10.2. *Apoptosis evaluation by flow cytometry*

After MDPC-23 cells were exposed to test materials for 3 days, the cells were washed with PBS to remove dead cell debris and remaining growth medium, detached with 0.05% trypsin–0.05 mM ethylenediamine tetra-acetic acid solution (pH 8.0) for 5 min, centrifuged and re-suspended at 1×10^4 cells/mL in 1× binding buffer (Biotium Inc). The cells were stained with fluorescein isothiocyanate (FITC)–annexin V (AnV; l_{abs}/l_{em} = 492/514 nm, green fluorescence) and ethidium homodimer-III (Etd; l_{abs}/l_{em} = 528/617 nm, red fluorescence) and incubated for 15 min in the dark. The stained cells were subjected to fluorescence-activated cell sorting (FACS) using a FACSCalibur flow cytometer (BD Biosciences, San Jose, CA, USA) to determine the percentage distribution of vital (AnV/Etd negative), early apoptotic (AnV positive, Etd negative), late apoptotic (secondary necrosis; AnV/Etd positive), and necrotic (AnV negative, Etd positive) cell populations.

3. Results

Fig. 1A represents the sol–gel reaction scheme using dimethyldiethoxysilane as the anchoring unit for the two

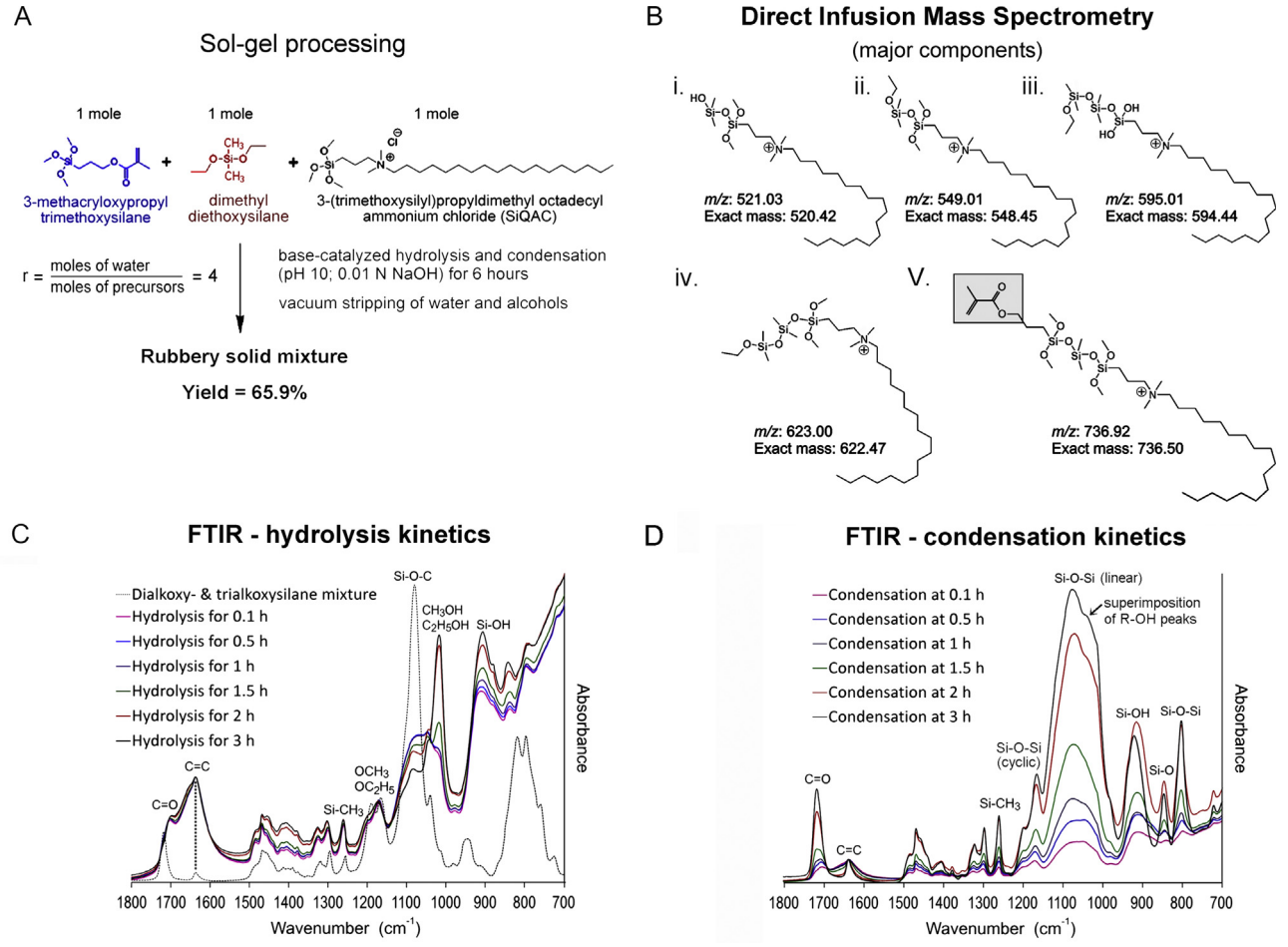

Fig. 1 – (A) Reaction scheme for synthesising DMDES-derived QAMS using dimethyldiethoxysilane as the anchoring unit. (B) Major quaternary ammonium containing component molecules (theoretical mass) produced by the sol–gel reaction corresponding to the major *m/z* (mass-to-charge ratio) peaks of the positive ions detected by direct infusion mass spectrometry. The molecule that can be copolymerised with the adhesive methacrylate comonomer blend is indicated by a box around its methacryloxy group. (C) Superimposition of the infrared spectra obtained from 0 to 3 h during sol–gel reaction between the dialkoxysilane and trialkoxysilane mixture, illustrating the hydrolysis kinetics of the reaction. (D) Superimposition of the infrared spectra obtained from 4 to 6 h during sol–gel reaction between the dialkoxysilane and trialkoxysilane mixture, illustrating the condensation kinetics of the reaction.

trialkoxysilanes, with a yield of 65.9 wt% following vacuum stripping of the water and alcohol reaction by-products. This organically modified silicate condensate was found to be soluble in HEMA, with the maximum concentration of the condensate in HEMA being 35 wt%. The major linear molecular components present in the condensate that contained quaternary ammonium species, as analysed by direct infusion mass spectrometry in the form of positive ions after electrospray ionisation, are shown in Fig. 1B. For the quaternary ammonium linear species, two of them represented the condensation between SIQAC and DMDES (i and ii in Fig. 1B), while the other 3 species (iii–v in Fig. 1B) represented the condensation products of the three alkoxysilanes. An unknown chemical (measured *m/z* 298.99) was also detected. The co-existence of quaternary ammonium silane species with (v in Fig. 1B) and without (i–iv in Fig. 1B) the methacryloxy functional group was also identified using DIMS. During the sol–gel reaction, the hydrolysis and condensation processes were monitored by ATR-FTIR. Fig. 1C and D shows the kinetics of hydrolysis and condensation of dialkoxysilane and trialkoxysilane mixture, respectively, by real-time ATR-FTIR. Hydrolysis was reflected by the decrease in the peak height of the Si–O–C band at 1082 cm^{-1}, increases of the alcohol peaks (CH_3OH and C_2H_5OH) between ~1016–1032 cm^{-1}, and the increase in the silanol (SiOH) peak at 912 cm^{-1} (Fig. 1C).[36] The extent of hydrolysis, although not complete, slowed down after 3 h, when peaks that were indicative of the condensation reaction began to appear. Condensation in base-catalysed sol–gel reactions proceed with the need for pH adjustment; the hydrolysis kinetics and condensation kinetics were presented separately only to facilitate interpretation. The condensation reaction that occurred from 4 to 6 h was represented by the increase of the major linear siloxane peak at ~1100 cm^{-1}, which corresponds to the symmetrical stretching mode of the Si–O–Si linkage (Fig. 1D).[36,37]

Proton NMR and carbon NMR spectra of the CD_3OD-solubilised, vacuum-stripped reaction products resulting from the sol–gel reaction are shown in Fig. 2A and B, respectively. Spectral data for ^1H NMR, δ (ppm): δ = 6.08 **H**CH=C(CO); 5.60 HC**H**=C(CO); 4.79 –OC**H**2–; 4.12 C**H**3–O–Si; 3.54–3.29 $N(CH_3)_2C\mathbf{H}_2$–CH_2; 3.16–3.13 $N(C\mathbf{H}_3)_2$; 1.92 $C\mathbf{H}_3C(CO)=CH_2$; 1.39 $C\mathbf{H}_2CH_2Si$; 1.28–1.22 $CH_3(C\mathbf{H}_2)_{16}$; 0.89 $C\mathbf{H}_3$-$(CH_2)_{17}$; 0.74–0.72 Si–$C\mathbf{H}_2$–; 0.17–0.14 $C\mathbf{H}_3$–Si. Spectral data for ^{13}C NMR, δ (ppm): δ = 168.4 **C**O(–O–)(C); 137.6 **C**$(CH_3)(CO)(CH_2)$; 126.1 **C**H_2=C; 67.5 –O**C**$H_2(CH_2$–); 65.5–64.6–N**C**$H_2(CH_2$–); 51.2–43.3 **C**H_3–O–Si; 33.0–23.7 $(CH_2)_{16}CH_3$; 18.7 **C**H_3–C=CH_2; 14.7 **C**H_3–$(CH_2)_{17}$;10.8–9.5 Si–**C**H_2**C**H_2; 1.5–0.9 Si(**C**$H_3)_2$. Solid-state silicon CP-MAS NMR spectrum of the rubbery solid produced after vacuum stripping revealed the presence of two series of peaks that are characteristic of siloxanes with trifunctional (T series) and difunctional structural units (D series).[38] Deconvolution of these peaks further identified the presence of T_3 and T_2 peaks in the T series, and D_2 and D_1 peaks in the D series (Fig. 2C). Spectral data for $^1H\rightarrow^{29}Si$

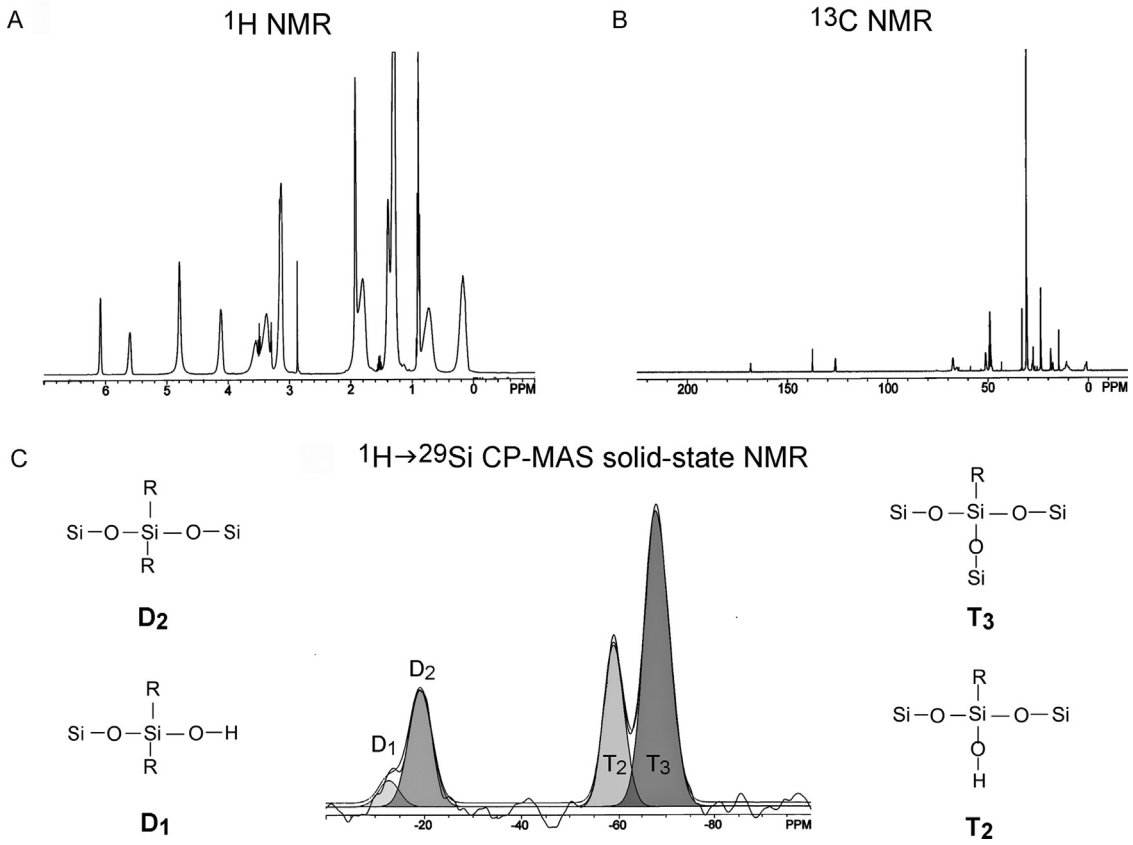

Fig. 2 – (A) ^1H NMR spectrum of water- and alcohol-depleted condensate of the DMDES-derived QAMS. (B) ^{13}C NMR spectrum of water- and alcohol-depleted condensate of the DMDES-derived QAMS. (C) $^1H\rightarrow^{29}Si$ CP MAS NMR spectrum of water- and alcohol-depleted condensate of the DMDES-derived QAMS showing D_1, D_2, T_2 and T_3 species.

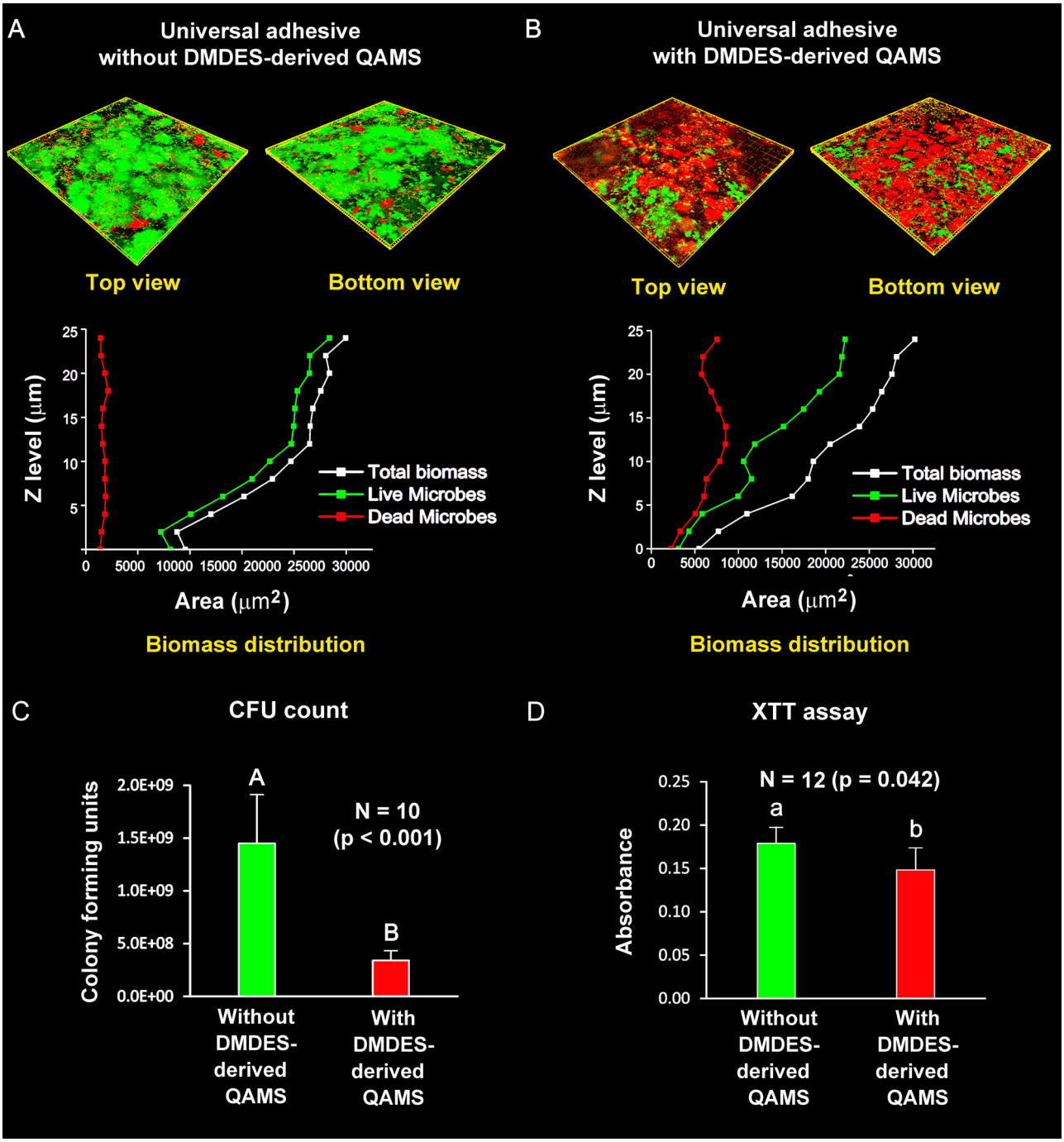

Fig. 3 – Confocal laser scanning microscopy images (2D overlay projections) of BacLight-stained 24-h *Streptococcus mutans* biofilms (live-green; dead-red) grown on polymerised universal adhesive disks. (A) Control universal adhesive without DMDES-derived-QAMS. (B) Antibacterial universal adhesive containing 7 wt% of DMDES-derived-QAMS. The chart beneath each image indicates the corresponding biomass of live and dead bacteria as a function of the biofilm level (Z step = 2 μm). (C) Colony forming unit (CFU) cell viability counts and (D) XTT cell metabolism assay of *S. mutans* grown on universal adhesive-coated dentine disks prepared using the control universal adhesive (0 wt% of DMDES-derived QAMS) and antibacterial universal adhesive (7 wt% of DMDES-derived QAMS). (For interpretation of the references to colour in this figure legend, the reader is referred to the web version of this article.)

CP-MAS NMR, δ (ppm): $\delta = -12.8$ D_1 (–SiO)**Si**(OH)$(CH_3)_2$; -19.2 D_2 $(\equiv SiO)_2$**Si**$(CH_3)_2$; -59.3 T_2 $(\equiv SiO)_2$**Si**(OH)R; -68.3 T_3 $(\equiv SiO)_3$**Si**R. T3:T2:D2:D1 = 100:45.2:36:2:7.0. Although the presence of the D series is indicative of the existence of linear molecules, identification of the T_3 siloxane structural unit provides evidence of some degree of 3-D network formation in the reaction products that are attributed to the two trialkoxysilanes.[39]

Fig. 3A and B shows stacked confocal images (top and bottom views) and the distribution of live/dead bacteria in *S. mutans* biofilms grown on the surfaces of representative adhesive-coated dentine disks derived from the control universal adhesive group and the antibacterial experimental universal adhesive group, respectively. For each Z-stack, the ''top view'' of the biofilm represents the 12th layer of the Z-stack which is 24 μm from the adhesive surface, while the ''bottom view'' of the biofilm represents the 1st layer of the Z-stack, which is 2 μm from the adhesive surface. Live bacteria that were stained only by the SYTO-9 component of the LIVE/DEAD® BacLight™ staining kit exhibited green fluorescence, while dead bacteria with damaged membranes were stained by both SYTO-9 and propidium iodide components and exhibited red fluorescence.[40] The relative area distributions of live and dead bacteria from the biomass at each level of a Z-stack are summarised in the line plots below the confocal images. From these line plots, it is apparent that the experimental universal adhesive that contained 7 wt% DMDES-derived QAMS possessed both initially contact-killing and release-killing capability prior to water-ageing. The CFU counts of live bacteria from *S. mutans* that retained the capability to produce colonies on further culturing are shown in Fig. 3C. The control universal adhesive group without DMDES-derived QAMS exhibited significantly higher CFU counts than the experimental universal adhesive group containing DMDES-derived QAMS ($p < 0.001$). Results of the XTT cell metabolism assay are shown in Fig. 3D. Bacteria derived from the control universal adhesive group exhibited significantly higher metabolic activity than those derived from the experimental universal adhesive group ($p < 0.05$).

Fig. 4A and C is representative TEM image of the use of the experimental universal adhesive for bonding to dentine in the etch-and-rinse mode or the self-etching mode, respectively. Similar to the control universal adhesive (not shown), application of the experimental universal adhesive in the etch-and-rinse mode after phosphoric acid etching resulted in a 5–7 μm thick hybrid layer that was devoid of remnant apatite crystallites (Fig. 4A). When employed for bonding to dentine in the etch-and-rinse mode, there was no significant difference in the microtensile bond strengths among the control and experimental versions of the universal adhesive, and the two commercially available universal adhesives, All-Bond Universal and Scotchbond Universal ($p = 0.313$; Fig. 4B). Similar to the control universal adhesive (not shown), application of the experimental universal adhesive in the self-etching mode to dentine resulted in a 300 nm thick, partially demineralised hybrid layer that contained remnant apatite crystallites (Fig. 4C). When employed for bonding to dentine in the self-etching mode, there was no significant difference in the microtensile bond strengths among the control and experimental versions of the universal adhesive, and the two commercially available universal adhesives, All-Bond Universal and Scotchbond Universal ($p = 0.286$; Fig. 4D).

Fig. 4E represents the plot of surface charge density/unit area of the quaternary ammonium species present on the QAMS-containing universal adhesive surface during a 3-month water-ageing period. The quantity of remnant quaternary ammonium species decreased during the first month and remained relatively stable until the end of three months. Fig. 4F shows the molar concentrations of N^+ species in the leachate derived from the QAMS-containing experimental universal adhesive disks during the 3-month water-ageing period. A burst release of QAMs could be seen during the first month. Thereafter, leaching of N^+ species was negligible until the end of the third month.

Fig. 5A is a schematic illustrating the experimental setup employed for examining the growth of *S. mutans* biofilm along a slice of the sectioned resin-dentine interface. After a 3-month water-ageing period, merged CLSM images of BacLight™-stained 24-h biofilms showed no visually apparent kill of the bacteria present in *S. mutans* biofilms grown on the resin-dentine interface created by the application of the control version of the universal adhesive in either the etch-and-rinse mode (Fig. 5B) or the self-etching mode (Fig. 5D). In the slice created by the use of the experimental version of the universal adhesive in the etch-and-rinse mode (Fig. 5C), a red fluorescence band could be seen along the adhesive-dentine interface that is indicative of the presence of dead bacteria along the base of the biofilm. A small amount of red fluorescence could also be identified in the composite-adhesive interface above, which could be attributed to the blending of the air-inhibition layer of the cured adhesive with the resin composite during polymerisation of the composite. The presence of live bacteria colonies growing on top of dead bacteria in the biofilm is suggestive of retained contact-killing potential following depletion of the leachable quaternary ammonium silane components after water-ageing. Similar features could be identified in the representative slice of the resin-dentine interface created by the use of the experimental version of the universal adhesive in the self-etching mode (Fig. 5E).

The relative cellular redox enzymatic activities of MPDC-23 odontoblast-like cells in response to indirect contact from the control and experimental versions of the universal adhesive are shown in Fig. 6A. There was no significant difference between the relative percentages of healthy cells in the control universal adhesive group ($86.5 \pm 3.7\%$) and in the experimental universal adhesive group ($84.8 \pm 3.2\%$) ($p > 0.05$). Results were semi-quantitative for the apoptosis/necrosis assay and were not statistically analysed (Fig. 6B). The percentage of cells with intact cell membranes (i.e. non-apoptotic and non-necrotic), after exposure to the control universal adhesive, was 51.0%. The percentage of the same category of vital cells after exposure to the experimental version of the universal adhesive was 65.6%. The percentage of vital cells in the negative control (untreated cells) was 93.5% instead of the expected 100%. This was probably due to alteration of membrane integrity during cell detachment by trypsinisation; trypsin caused disruption of fibronectin–integrin interaction between cells, while EDTA chelated calcium ions required for promoting fibronectin–integrin interactions. Two-dimensional plots of the distribution of sorted vital, early apoptotic, late apoptotic and necrotic cells are shown in Fig. 6C for the control universal adhesive, Fig. 6D for the experimental universal adhesive, Fig. 6E for the IRM positive control, and Fig. 6F for the untreated cells that had not been exposed to test materials.

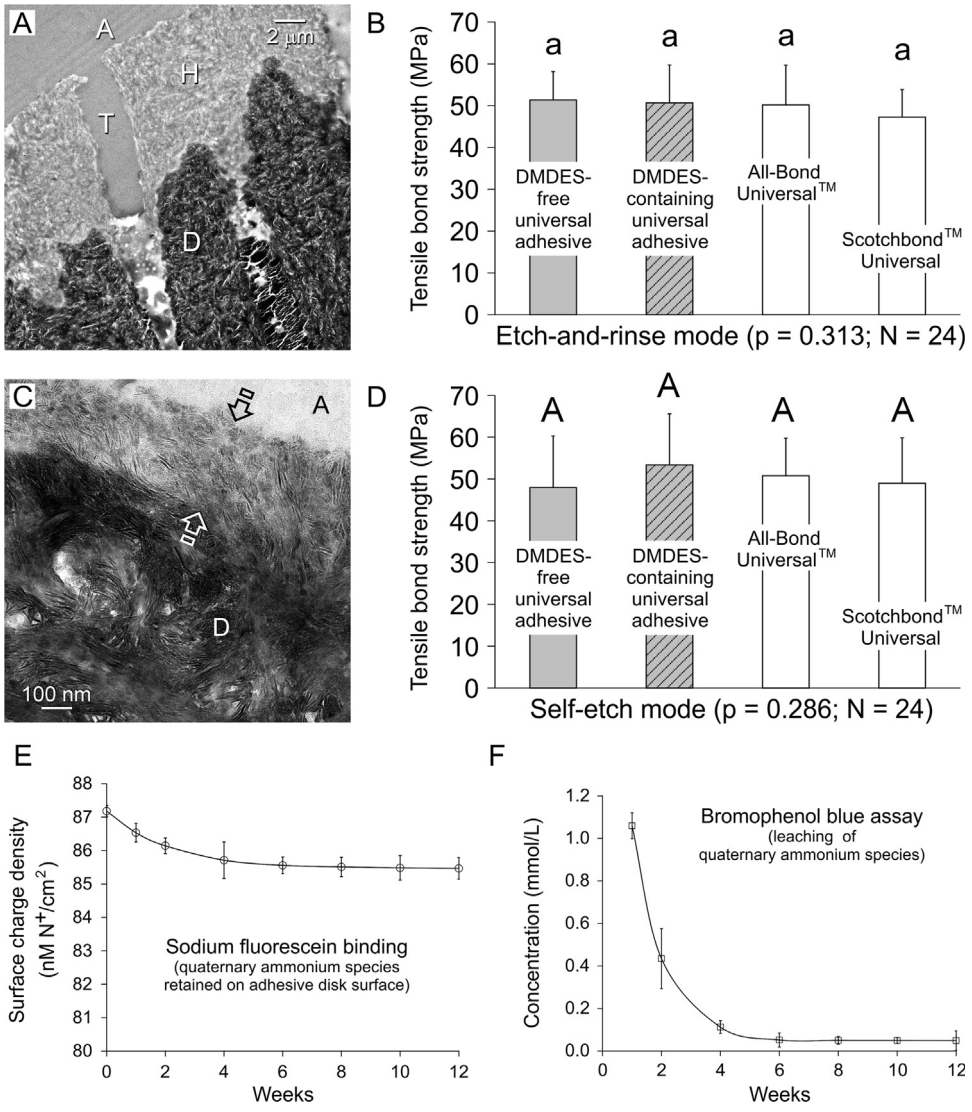

Fig. 4 – Representative transmission electron micrographs of adhesive-dentine interface and microtensile bond strength results from coronal dentine bonded with the control universal adhesive or the antibacterial universal adhesive in etch-and-rinse mode (A and B) or self-etch mode (C and D). For microtensile bond strength, the data were compared with two commercially available, non-antibacterial universal adhesives. Abbreviations for micrographs – A: adhesive; D: dentine; H: hybrid layer; T: dentinal tubule; open arrows: hybrid layer. (E) Sodium fluorescein binding assay for examining the amount of remnant quaternary sammonium charges present on the surface of adhesive disks prepared with the antibacterial universal adhesive during a 12-week water-ageing period. (F) Bromophenol blue assay depicting the amount of quaternary ammonium moieties present in the leachate after the antibacterial universal adhesive disks were stored in deionised water for 12 weeks.

4. Discussion

Statistically, replacement of previously placed dental restorations consumes more than half of the restorative dentistry procedures performed in general dental practices.[41,42] Direct resin composite restorations have higher failure rates and increased frequency of replacement when compared with direct amalgam restorations and indirect ceramic restorations.[43–45] The contributing factors to premature failures in direct resin composite restorations include stresses produced by polymerisation shrinkage of resin composites along cavity walls,[46] and the tendency for more biofilms to be accumulated on the surface of these restorations.[47] These premature failures are initiated predominantly by secondary caries along the restorative margins.[48] The adhesive-dentine interface has been considered the weak link in resin composite restorations, particularly in hard-to-access cervical margins in proximal boxes of large Class II cavities.[49] Bacteria leakage is a common occurrence along the adhesive-dentine interface that leads to secondary caries and pulpal inflammation.[50] *S. mutans*, being one of the early colonisers of dental plaque,[51] is a major contributor to the virulence of mixed cariogenic biofilms.[52,53] Cariogenic bacteria produce enzymes that degrade resin

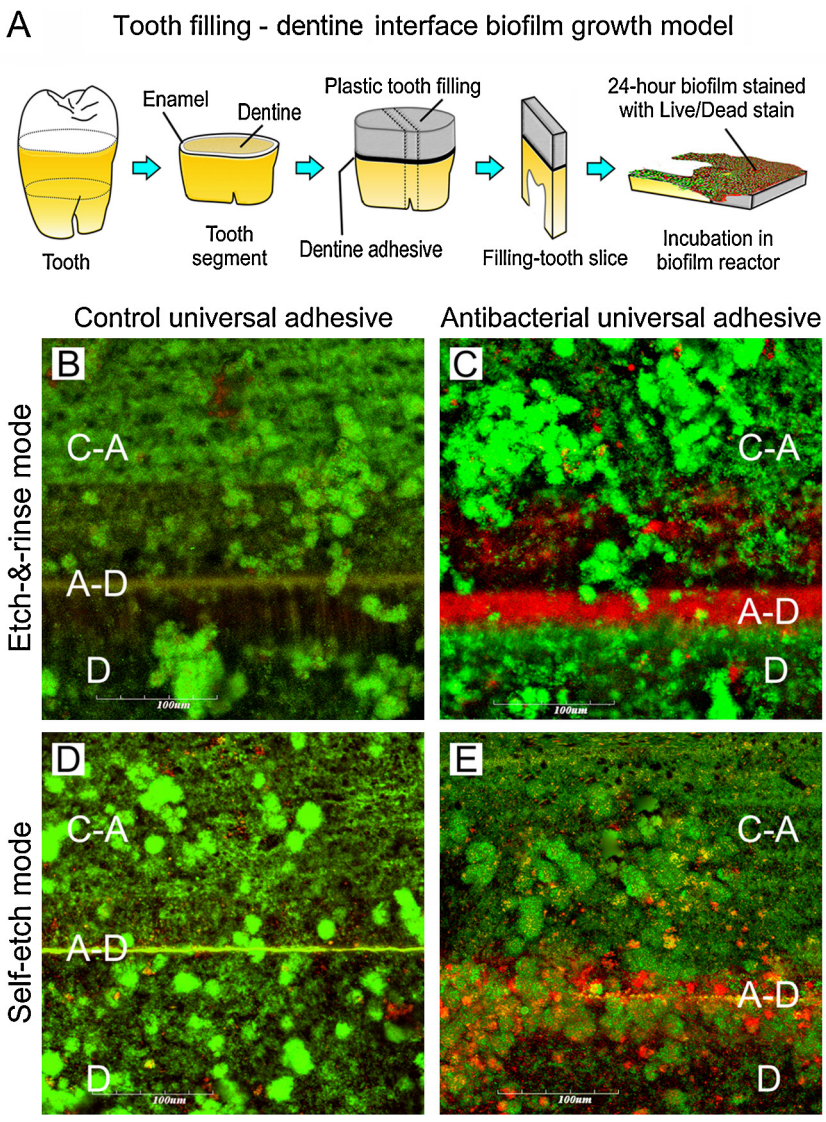

Fig. 5 – (A) Schematic representation of the experimental setup employed for the tooth filling-dentine interface biofilm growth model. (B–E) Confocal laser scanning microscopy merged images of BacLight™-stained 24-h *S. mutans* biofilms (live-green; dead-red) grown on slices of the resin-dentine interface that had been aged in water for 3 months. *Abbreviations*: C-A: composite-adhesive; A-D: adhesive-dentine interface; D: coronal dentine. For the slices prepared using the antibacterial experimental universal adhesive in the etch-and-rinse mode (C) or the self-etch mode (E), live bacteria colonies can be seen growing on top of dead bacteria within the biofilms. (For interpretation of the references to colour in this figure legend, the reader is referred to the web version of this article.)

composites and dentine adhesives,[54] thereby exacerbating bacteria leakage along the adhesive-dentine interface.[55] Thus, development of antimicrobial dentine adhesives represents a logical approach for controlling secondary caries along the tooth-restorative margins.[56]

Based on the ecological plaque hypothesis,[57,58] antimicrobial agents incorporated into oral health care products are required to meet the apparently contradictory requirements of maintaining plaque biofilms at levels compatible with oral health, but without disrupting the natural microbial ecology of the mouth that causes the overgrowth of opportunistic pathogens.[59] At concentrations above the minimum inhibitory concentration, antimicrobial agents should possess the ability to eradicate biofilms and/or kill disease-associated bacteria. Even when the concentrations of these antimicrobial agents are subsequently reduced to sub-lethal concentrations, they should still exert beneficial effects by inhibiting traits associated with bacterial pathogenicity.[59] From the perspective of antimicrobial adhesives, it appears that materials possessing both release-killing and contact-killing capabilities have better potential to meet these requirements than those possessing contact-killing capability only. Among the plethora of antimicrobial agents available for oral health care, quaternary ammonium methacrylates appear to be good candidates for incorporation into dentine adhesives because these antibacterial resin momomers can copolymerise with

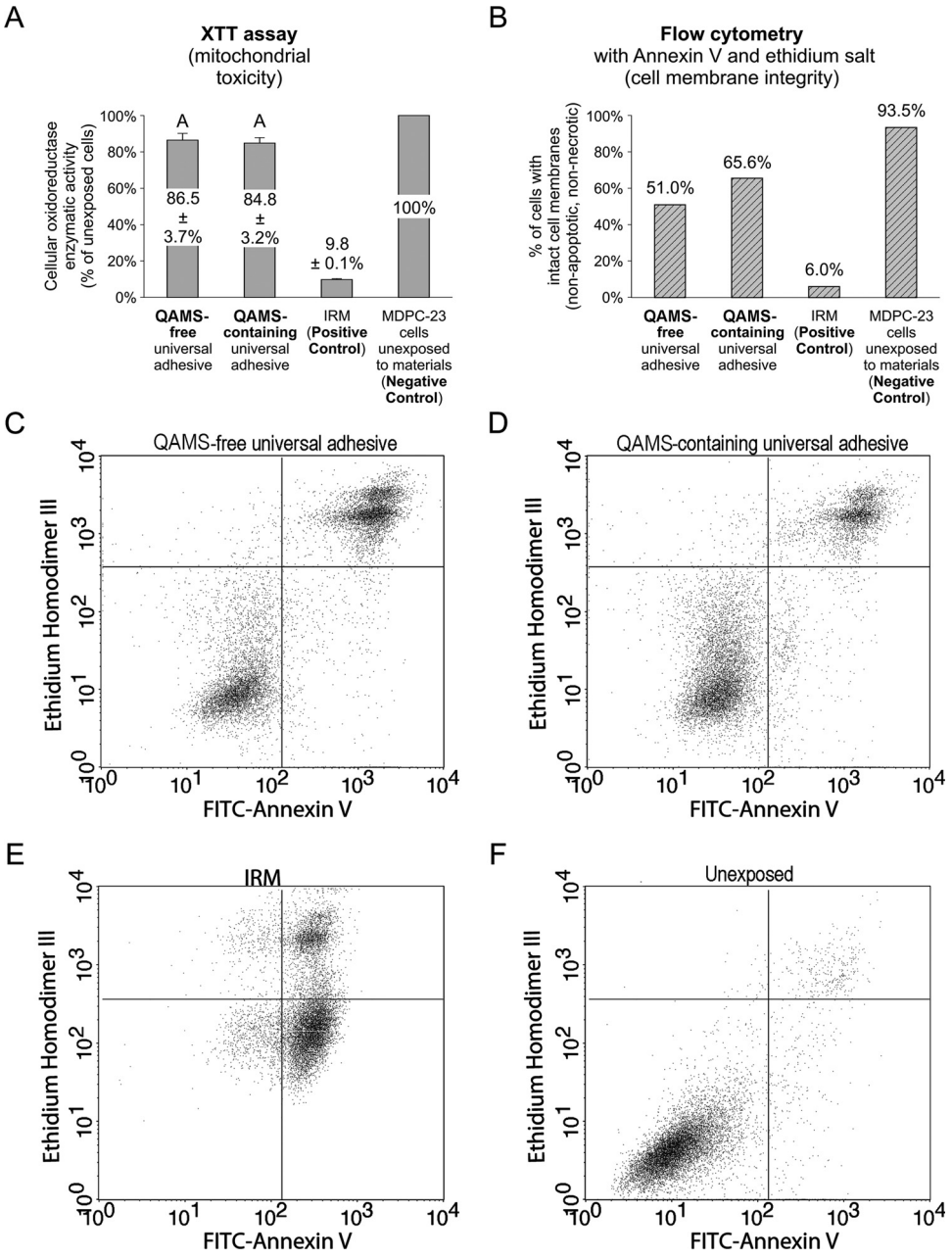

Fig. 6 – Cytotoxicity evaluations using a rat odontoblast-like cell line. (A) XTT assay. (B) Flow cytometry examination of apoptosis/necrosis. (C–F) Two-dimensional annexin V-ethidium homodimer III plots of the distribution of sorted vital, early apoptotic, late apoptotic and necrotic cells in (C). Control universal adhesive without DMDES-derived QAMS. (D) Experimental universal containing DMDES-derived QAMS. (E) IRM positive control. (F) Unexposed cells negative control.

other dental monomers. Apart from their antimicrobial activities, quaternary ammonium methacrylates also inhibit dentine-bound matrix metalloproteinases that are responsible for the degradation of the water-rich, resin-sparse collagen network in hybrid layers created by etch-and-rinse dentine adhesives.[60]

To date, the only quaternary ammonium methacrylate resin monomer that has been incorporated into a commercial self-etching primer system is 12-methacryloyloxy dodecylpyridinium bromide (MDPB).[61,62] Known as Clearfil SE Protect (Kuraray Medical Inc., Tokyo, Japan), the MPDB-containing self-etching primer has been shown to reduce growth of *S. mutans* biofilms based on a contact-killing mechanism.[63,64] Other antibacterial quaternary ammonium methacrylates have been synthesised and incorporated into etch-and-rinse adhesive formulations.[65–70] Because copolymerisation of quaternary ammonium methacrylates with adhesive resin monomers produces antibacterial polymer matrices with only contact-killing capability on the polymerised adhesive surface,[67,70] dental researchers have adopted a bimodal antimicrobial strategy developed in other biomedical fields,[6] by incorporating silver nanoparticles into experimental

quaternary ammonium methacrylate-containing etch-and-rinse adhesives. The use of this bimodal antimicrobial strategy augmented the bactericidal effects of those experimental adhesives via a combination of contact-killing and release-killing modes.[71,72] Nanosilver, one of the earliest developed nanotechnology products, has found extensive commercial applications in consumer products, ranging from wound dressings, antibacterial textiles to baby products. Nanosilver is a versatile antimicrobial agent that has proven efficacy against bacteria, yeast, fungi, algae and viruses.[73,74] Nevertheless, the antimicrobial activity of nanosilver is inconsistent in that some bacteria appear to develop resistance to nanosilver upon prolonged exposure. For example, nanosilver effectively suppressed the growth of the clinical pathogen *Escherichia coli*; however, prolonged nanosilver exposure resulted in the development of silver-tolerant *Bacillus* species that proliferate abnormally to dominate the microbiota.[75] Another issue that has become an escalating concern is the potential cytotoxicity associated with silver at the nanoscale. Historical and anecdotal records of colloidal silver have often been used as empirical proof of the low toxicity of nanosilver. Despite the widespread use of nanosilver commercial products, very few studies have attempted to examine the biological effects of nanosilver exposure. Although silver is biochemically inert and biocompatible in bulk, several studies that employed contemporary standards of toxicological assessment reported significant toxicity of nanosilver to mammalian cells. Exposure to nanosilver resulted in decrease in mitochondrial function and induction of apoptosis in different mammalian cell lines.[76–79] In a recent conference report, characterisation of silver nanoparticles in complex matrices has been regarded as a challenge which may adversely hinder future application of nanosilver as an antibacterial agent.[80]

Because consumer exposure scenarios to nanosilver are only beginning to emerge and progress in the identification of silver-resistant bacteria strains is only in an infancy stage, the authors attempted to avoid such potential complications by adopting an alternative bimodal antimicrobial strategy for formulating antimicrobial dentine adhesives. Understandably, there are more precise ''grafting from'' chemical modification techniques such as reversible addition fragmentation chain transfer polymerisation (RAFT), atom transfer radical polymerisation (ATRP), or nitroxide-mediated polymerisation that enable controlled attachment of an antimicrobial functionality to specific sites of organic molecules, with appreciably high yields.[81–83] Nevertheless, a facile one-pot sol–gel processing technique was used in the present work to generate, without additional purification, a series of molecules that contain the quaternary ammonium functionality with the antibacterial 18-carbon alkyl chain (Fig. 1B). Since quaternary ammonium silanes (QAS) do not possess methacryloxy functional groups, they may be trapped within the polymerised adhesive matrix and diffuse slowly out of the matrix after water sorption to achieve a releasing-kill effect. On the contrary, QAMS can copolymerise with the adhesive polymer matrix and provides long-term antimicrobial activity via a non-leaching, contact-killing mechanism. In the present work, identification of the products of the sol–gel reaction was accomplished using positive ions generated by electrospray ionisation and direct infusion mass spectrometry. Since molecules containing quaternary ammonium silane have the tendency to bind to substrate surfaces, there is a possibility that analysis is incomplete because some of the molecules may have been chemically bound to the source needle. Future work should aim at identification of the molecular spectrum of the sol–gel reaction products via matrix-assisted laser desorption ionisation, and analysing the components via a time-of-flight mass spectrometer (MALDI-TOF). This is because the MALDI-TOF mass spectrometry technique has been reported to be successful in the analysis of complex organosilanes.[84,85]

In previous work on antimicrobial adhesives, the antimicrobial agents were incorporated into either self-etching primers or etch-and-rinse adhesives. Universal adhesives that enable clinicians to choose between an etch-and-rinse mode or self-etching mode for bonding to tooth substrates are rapidly gaining acceptance, as evidenced by the introduction of five commercial products over the last couple of years (All Bond Universal; Scotchbond Universal Adhesive; Prime&Bond Elect, Dentsply Caulk, Milford, DE, USA; Futurebond U, Voco GmbH, Cuxhaven, Germany; and Clearfil Universal Bond, Kuraray Medical Inc., Tokyo, Japan). Thus, DMDES-derived QAMS and the accompanying quaternary ammonium silane sol–gel reaction products were incorporated into an experimental universal adhesive formulation in the present study. A potential advantage of using these molecules over the use of quaternary ammonium methacrylates is that they contain pendant silanol groups that can chemically bond to glass and silica fillers employed in some dentine adhesives. Incorporation of molecules containing siloxane linkages (Fig. 1B) into a brittle polymerised resin blend may also impart flexibility to the polymerised adhesive without sacrificing other useful properties, due to the bending flexibility of the Si–O–Si bond angle.[86] This may enable the polymerised adhesive to dissipate polymerisation stresses more effectively. However, this property was not evaluated in the present work as composite placement was performed on flat bonded dentine surfaces with a favourable cavity geometry factor to facilitate microtensile bond testing. This property should be examined in future studies. Nevertheless, the microtensile bond strength results derived from the control and antibacterial version of the universal adhesive (Fig. 4B and D) validated the first hypothesis tested, in that incorporation of DMDES-derived QAMS into an experimental universal adhesive does not compromise the bond strength of the adhesive to dentine when it is used in the etch-and-rinse mode or the self-etching mode.

In the present study, CLSM, CFU counts and XTT assay were used to evaluate the initial bactericidal activities of DMDES-derived QAMS-containing adhesive. Confocal imaging indicated that killing of bacteria in *S. mutans* biofilms was not confined only to the substrate surface, but could also be identified from the bulk of the biofilms (Fig. 3A). The CFU counts quantified viable bacteria present within the biofilms after the latter were detached from the adhesive-coated dentine disks (Fig. 3C). The XTT assay quantified the intracellular mitochondrial dehydrogenase activities of live bacteria present in the biofilms (Fig. 3D). Taken together, these results are confirmative of the dual biocidal modes of the antibacterial adhesive. For the 3-month ageing experiments,

the bromophenol blue assay revealed there was release of leachable quaternary ammonium species during the water-ageing period (Fig. 4F). This result supports that the leaching of unbound quaternary ammonium species was responsible for microbes at a distance from the adhesive surface during the initial period of CLSM imaging. Fluorescein staining identified that positive-charged quaternary ammonium groups were retained on the adhesive surfaces after 3 months of water-ageing (Fig. 4E). The data is consistent with the 3-month CLSM imaging results (Fig. 5), indicating that immobilised QAMS within the adhesive could provide long-term antibacterial activity predominantly by contact-killing. A slice of the resin-dentine interface was employed for the 3-month CLSM imaging to determine if antimicrobial activity was retained when the adhesive existed as a thin layer, such as that present along cavosurface margins. The observation of biofilm inhibition in a sectioned resin-dentine interface further suggests that the adhesive still possesses contact-killing ability after it is worn down, for example, by aggressive tooth brushing. Taken together, the results validated the second hypothesis tested, in that inclusion of a blend of quaternary ammonium species with and without methacryloxy functional group created by one-pot sol–gel processing within the experimental universal adhesive results in both initial release-killing and retained contact-killing activity in the resin-dentine interface against *S. mutans* biofilms after 3 months of water-ageing.

Cytotoxicity tests are integral in safety evaluations of products contacting with human tissues. Admittedly, limitations exist for cell culture models; nevertheless, they provide critical information prior to implementation of more labour-intensive in vivo studies using small and large animal models. Two complementary strategies were employed in the present study to examine the cell viability in the presence of the antibacterial universal adhesive; both strategies have their merits and limitations. The first strategy (XTT assay; Fig. 6A) evaluated cell metabolic activity, based on the premise that dead cells are incapable of metabolising tetrazolium salts via oxidoreductase activities involved in the citric acid cycle and the electron transport chain. Similar assays such as the MTT (3-[4,5-dimethylthiazol-2-yl]-2,5 diphenyl tetrazolium bromide) assay were employed in previous studies for evaluation of the cytotoxicity of antibacterial adhesives.[68,70,72] Although such cell metabolism assays provide information on one aspect of cytotoxicity, it is known that dentine adhesive monomers induce cellular damage via apoptosis.[87,88] Such a process was not evaluated by the aforementioned assays. Cellular damage invariably results in the loss of the ability of the cell to provide energy for cell function and growth. Apoptosis is an active mode of cell death that relies on sustained energy production from cell metabolism for its induction.[89] The use of tetrazolium salt-based assays alone may have underestimated cellular damage and detect cell death only at the later stage of apoptosis when cellular metabolism is substantially reduced. It is also critical that the inclusion of antimicrobial components to dentine adhesives does not further intensify the apoptosis-inducing potential of the antimicrobial adhesives. Thus, a second strategy was employed in the present study to examine the potential of the antibacterial adhesive to induce apoptosis, using fluorescent dyes that examined plasma membrane alterations (permeability) induced by cellular damage (Fig. 6B). Based on the results from the two cytotoxicity assays, it is reasonable to assert that inclusion of antimicrobial components utilised in the present study does not adversely affect the cytotoxicity of the universal dentine adhesive formulation.

5. Conclusions

A facile method is introduced for one-pot synthesis of antibacterial quaternary ammonium silane and quaternary ammonium methacryloxy silane monomers using a sol–gel route. When these monomers are incorporated into a universal dentine adhesive, the antibacterial adhesive version kills bacteria in *S. mutans* biofilms not only through the release of leachable quaternary ammonium species, but also via immobilised quaternary ammonium methacryloxy silane within the resin-dentine interface. The DMDES-derived QAMS-containing universal adhesive has similar tensile bond strength as two commercially available universal adhesives when it is used for bonding to dentine in the etch-and-rinse mode and self-etching mode. Because quaternary ammonium-containing resins have the potential to prevent collagen degradation in dentine hybrid layers, the potential of the experimental antimicrobial universal adhesive developed in the present work in maintaining the longevity of resin-dentine bonds should be examined in future studies.

Acknowledgements

The authors thank Dr. YaShen, Division of Endodontics, Faculty of Dentistry, The University of British Columbia, Canada for preparing the CLSM stacked images in Fig. 3A and B, and Mrs. Michelle Barnes for secretarial support.

REFERENCES

1. Timofeeva L, Kleshcheva N. Antimicrobial polymers: mechanism of action, factors of activity, and applications. *Applied Microbiology and Biotechnology* 2011;**89**:475–92.
2. Siedenbiedel F, Tiller JC. Antimicrobial polymers in solution and on surfaces: overview and functional principles. *Polymers* 2012;**4**:46–71.
3. Ferreira L, Zumbuehl A. Non-leaching surfaces capable of killing microorganisms on contact. *Journal of Materials Chemistry* 2009;**19**:7796–806.
4. Ho CH, Tobis J, Sprich C, Thomann R, Tiller JC. Nanoseparated polymeric networks with multiple antimicrobial properties. *Advanced Materials* 2004;**16**:957–61.
5. Sambhy V, MacBride MM, Peterson BR, Sen A. Silver bromide nanoparticle/polymer composites: dual action tunable antimicrobial materials. *Journal of the American Chemical Society* 2006;**128**:9798–808.
6. Li Z, Lee D, Sheng XX, Cohen RE, Rubner MF. Two-level antibacterial coating with both release-killing and contact-killing capabilities. *Langmuir* 2006;**22**:9820–3.
7. Isquith AJ, Abbott EA, Walters PA. Surface-bonded antimicrobial activity of an organosilicon quaternary ammonium chloride. *Applied Microbiology* 1972;**24**:859–63.

8. Battice DR, Hales MG. A new technology for producing stabilized foams having antimicrobial activity. *Journal of Cellular Plastics* 1985;**21**:332–7.
9. Murray PR, Niles AC, Heeren RL. Microbial inhibition on hospital garments treated with Dow Corning 5700 antimicrobial agent. *Journal of Clinical Microbiology* 1988;**26**:1884–6.
10. Gottenbos B, van der Mei HC, Klatter F, Nieuwenhuis P, Busscher HJ. In vitro and in vivo antimicrobial activity of covalently coupled quaternary ammonium silane coatings on silicone rubber. *Biomaterials* 2002;**23**:1417–23.
11. Oosterhof JJ, Buijssen KJ, Busscher HJ, van der Laan BF, van der Mei HC. Effects of quaternary ammonium silane coatings on mixed fungal and bacterial biofilms on tracheoesophageal shunt prostheses. *Applied and Environmental Microbiology* 2006;**72**:3673–7.
12. Song L, Baney RH. Antibacterial evaluation of cotton textile treated by trialkoxysilane compounds with antimicrobial moiety. *Textile Research Journal* 2010;**81**:504–11.
13. Yuen JWM, Yung JYK. Medical implications of antimicrobial coating polymers – organosilicon quaternary ammonium chloride. *Modern Chemistry & Applications* 2013;**1**:107. http://dx.doi.org/10.4172/2329-6798.1000107.
14. Blizzard JD, Kimmerling K, Rapp JP. Two- and three-component siloxanes and related compounds and compositions. United States Patent Application 2013; US 20130230676 A1.
15. Mackenzie JD. Sol–gel research – achievements since 1981 and prospects for the future. *Journal of Sol Gel Science and Technology* 2003;**26**:237.
16. Innocenzi P, Brusotin G, Guglielmi M, Bertani R. New synthetic route to (3-glycidoxypropyl)triethoxysilane-based hybrid organic–inorganic materials. *Chemistry of Materials* 1999;**11**:1672–9.
17. Schottner G. Hybrid sol–gel-derived polymers: applications of multifunctional materials. *Chemistry of Materials* 2000;**13**:3422–35.
18. Gong SQ, Epasinghe J, Rueggeberg FA, Niu LN, Mettenberg D, Yiu CKY, *et al.* An ORMOSIL-containing orthodontic acrylic resin with concomitant improvements in antimicrobial and fracture toughness properties. *PLOS ONE* 2012;**7**:e42355.
19. Gong SQ, Niu LN, Kemp LK, Yiu CKY, Ryou H, Qi YP, *et al.* Quaternary ammonium silane-functionalized, methacrylate resin composition with antimicrobial activities and self-repair potential. *Acta Biomaterialia* 2012;**8**:3270–82.
20. Andreasson H, Boman A, Johnsson S, Karlsson S, Barregård L. On permeability of methyl methacrylate, 2-hydroxyethyl methacrylate and triethyleneglycol dimethacrylate through protective gloves in dentistry. *European Journal of Oral Science* 2003;**111**:529–35.
21. Tay FR, Gwinnett AJ, Wei SH. The overwet phenomenon: a transmission electron microscopic study of surface moisture in the acid-conditioned, resin–dentin interface. *American Journal of Dentistry* 1996;**9**:161–6.
22. Spencer P, Wang Y. Adhesive phase separation at the dentin interface under wet bonding conditions. *Journal of Biomedical Materials Research* 2001;**62**:447–56.
23. Abedin F, Ye Q, Good HJ, Parthasarathy R, Spencer P. Polymerization- and solvent-induced phase separation in hydrophilic-rich dentin adhesive mimic. *Acta Biomaterialia* 2014. [Epub ahead of print].
24. Van Landuyt KL, De Munck J, Snauwaert J, Coutinho E, Poitevin A, Yoshida Y, *et al.* Monomer-solvent phase separation in one-step self-etch adhesives. *Journal of Dental Research* 2005;**84**:183–8.
25. Liu R, Xu Y, Wu D, Sun Y, Gao H, Yuan H, *et al.* Comparative study on the hydrolysis kinetics of substituted ethoxysilanes by liquid-state ^{29}Si NMR. *Journal of Non-Crystalline Solids* 2004;**343**:61–70.
26. Xu Y, Sun X, Wu D, Sun Y, Yang Y, Yuan H, *et al.* Ammonia catalyzed hydrolysis-condensation kinetics of tetraethoxysilane/dimethyldiethoxysilane mixtures studied by ^{29}Si NMR and SAXS. *Journal of Solution Chemistry* 2007;**36**:327–44.
27. De Witte BM, Comrners D, Uytterhoeven JB. Distribution of organic groups in silica gels prepared from organo-alkoxysilanes. *Journal of Non-Crystalline Solids* 1996;**202**:35–41.
28. Muñoz MA, Luque I, Hass V, Reis A, Loguercio AD, Bombarda NH. Immediate bonding properties of universal adhesives to dentine. *Journal of Dentistry* 2013;**41**:404–11.
29. Perdigão J, Loguercio AD. Universal or multi-mode adhesives: why and how? *Journal of Adhesive Dentistry* 2014;**16**:193–4.
30. Perdigão J, Kose C, Mena-Serrano AP, De Paula EA, Tay LY, Reis A, *et al.* A new universal simplified adhesive: 18-month clinical evaluation. *Operative Dentistry* 2014;**39**:113–27.
31. Tay FR, Moulding KM, Pashley DH. Distribution of nanofillers from a simplified-step adhesive in acid-conditioned dentin. *Journal of Adhesive Dentistry* 1999;**1**:103–17.
32. Tiller JC, Liao CJ, Lewis K, Klibanov AM. Designing surfaces that kill bacteria on contact. *Proceedings of the National Academy of Sciences of the United States of America* 2001;**98**:5981–5.
33. Yamamoto K. Sensitive determination of quaternary ammonium salts by extraction-spectrophotometry of ion associates with bromophenol blue anion and coextraction. *Analytica Chimica Acta* 1995;**302**:75–9.
34. Bouillaguet S, Virgillito M, Wataha J, Ciucchi B, Holz J. The influence of dentine permeability on cytotoxicity of four dentine bonding systems, in vitro. *Journal of Oral Rehabilitation* 1998;**25**:45–51.
35. Hanks CT, Sun ZL, Fang DN, Edwards CA, Wataha JC, Ritchie HH, *et al.* Cloned 3T6 cell line from CD-1 mouse fetal molar dental papillae. *Connective Tissue Research* 1998;**37**:233–49.
36. Leyden DE, Shreedhara Murthy RS, Blitz JP, Atwater JB, Rachetti A. Reflectance FTIR investigations of the reactions of silanes on silica surfaces. *Microchimica Acta (Wien)* 1988;**11**:53–6.
37. Rubio F, Rubio J, Oteo JL. A FT-IR study of the hydrolysis of tetraethylorthosilicate (TEOS). *Spectroscopy Letters* 1998;**31**:199–219.
38. Su K, DeGroot Jr JV, Norris AW, Lo PY. Siloxane materials for optimal applications. *Proceedings of SPIE* 2005;**6029**:60291C. http://dx.doi.org/10.1117/12.667752.
39. Brinker CJ, Scherer GW. Sol–Gel Science, the Physics and Chemistry of Sol–Gel Processing. San Diego: Academic Press; 1990.
40. Boulos L, Prévost M, Barbeau B, Coallier J, Desjardins R. LIVE/DEAD BacLight: application of a new rapid staining method for direct enumeration of viable and total bacteria in drinking water. *Journal of Microbiological Methods* 1999;**37**:77–86.
41. Deligeorgi V, Mjör IA, Wilson NH. An overview of reasons for the placement and replacement of restorations. *Primary Dental Care* 2001;**8**:5–11.
42. Gordan VV, Riley 3rd JL, Geraldeli S, Rindal DB, Qvist V, Fellows JL, *et al.* Repair or replacement of defective restorations by dentists.The Dental Practice-Based Research Network. *Journal of the American Dental Association* 2012;**143**:593–601.
43. Manhart J, Chen H, Hamm G, Hickel R. Buonocore Memorial Lecture Review of the clinical survival of direct and indirect restorations in posterior teeth of the permanent dentition. *Operative Dentistry* 2004;**29**:481–508.
44. Soncini JA, Maserejian NN, Trachtenberg F, Tavares M, Hayes C. The longevity of amalgam versus compomer/composite restorations in posterior primary and permanent

teeth: findings From the New England Children's Amalgam Trial. *Journal of the American Dental Association* 2007;**138**:763–72.
45. Sunnegårdh-Grönberg K, van Dijken JW, Funegård U, Lindberg A, Nilsson M. Selection of dental materials and longevity of replaced restorations in Public Dental Health clinics in northern Sweden. *Journal of Dentistry* 2009;**37**:673–8.
46. Ferracane JL. Buonocore Lecture. Placing dental composites – a stressful experience. *Operative Dentistry* 2008;**33**:247–57.
47. Beyth N, Domb AJ, Weiss EI. An in vitro quantitative antibacterial analysis of amalgam and composite resins. *Journal of Dentistry* 2007;**35**:201–6.
48. Bernardo M, Luis H, Martin MD, Leroux BG, Rue T, Leitão J, *et al*. Survival and reasons for failure of amalgam versus composite posterior restorations placed in a randomized clinical trial. *Journal of the American Dental Association* 2007;**138**:775–83.
49. Spencer P, Ye Q, Park J, Topp EM, Misra A, Marangos O, *et al*. Adhesive/dentin interface: the weak link in the composite restoration. *Annals of Biomedical Engineering* 2010;**38**: 1989–2003.
50. Bergenholtz G, Cox CF, Loesche WJ, Syed SA. Bacterial leakage around dental restorations: its effect on the dental pulp. *Journal of Oral Pathology* 1982;**11**:439–50.
51. Marsh PD. Dental plaque as a microbial biofilm. *Caries Research* 2004;**38**:204–11.
52. Kuramitsu HK, Wang BY. The whole is greater than the sum of its parts: dental plaque bacterial interactions can affect the virulence properties of cariogenic *Streptococcus mutans*. *American Journal of Dentistry* 2011;**24**:153–4.
53. Koo H, Falsetta ML, Klein MI. The exopolysaccharide matrix: a virulence determinant of cariogenic biofilm. *Journal of Dental Research* 2013;**92**:1065–73.
54. Bourbia M, Ma D, Cvitkovitch DG, Santerre JP, Finer Y. Cariogenic bacteria degrade dental resin composites and adhesives. *Journal of Dental Research* 2013;**92**:989–94.
55. Kermanshahi S, Santerre JP, Cvitkovitch DG, Finer Y. Biodegradation of resin-dentin interfaces increases bacterial microleakage. *Journal of Dental Research* 2010;**89**:996–1001.
56. Imazato S, Ma S, Chen JH, Xu HH. Therapeutic polymers for dental adhesives: loading resins with bio-active components. *Dental Materials* 2014;**30**:97–104.
57. Marsh PD. Microbial ecology of dental plaque and its significance in health and disease. *Advances in Dental Research* 1994;**8**:263–71.
58. Takahashi N, Nyvad B. The role of bacteria in the caries process: ecological perspectives. *Journal of Dental Research* 2011;**90**:294–303.
59. Marsh PD. Controlling the oral biofilm with antimicrobials. *Journal of Dentistry* 2010;**38**(Suppl. 1):S11–5.
60. Tezvergil-Mutluay A, Agee KA, Uchiyama T, Imazato S, Mutluay MM, Cadenaro M, *et al*. The inhibitory effects of quaternary ammonium methacrylates on soluble and matrix-bound MMPs. *Journal of Dental Research* 2011;**90**: 535–40.
61. Imazato S, Kinomoto Y, Tarumi H, Ebisu S, Tay FR. Antibacterial activity and bonding characteristics of an adhesive resin containing antibacterial monomer MDPB. *Dental Materials* 2003;**19**:313–9.
62. Imazato S, Tay FR, Kaneshiro AV, Takahashi Y, Ebisu S. An in vivo evaluation of bonding ability of comprehensive antibacterial adhesive system incorporating MDPB. *Dental Materials* 2007;**23**:170–6.
63. Carvalho FG, Puppin-Rontani RM, Fúcio SB, Negrini Tde C, Carlo HL, Garcia-Godoy F. Analysis by confocal laser scanning microscopy of the MDPB bactericidal effect on *S. mutans* biofilm CLSM analysis of MDPB bactericidal effect on biofilm. *Journal of Applied Oral Sciences* 2012;**20**:568–75.
64. Brambilla E, Ionescu A, Fadini L, Mazzoni A, Imazato S, Pashley D, *et al*. Influence of MDPB-containing primer on *Streptococcus mutans* biofilm formation in simulated Class I restorations. *Journal of Adhesive Dentistry* 2013;**15**:431–8.
65. Li F, Chai ZG, Sun MN, Wang F, Ma S, Zhang L, *et al*. Anti-biofilm effect of dental adhesive with cationic monomer. *Journal of Dental Research* 2009;**88**:372–6.
66. Xiao YH, Ma S, Chen JH, Chai ZG, Li F, Wang YJ. Antibacterial activity and bonding ability of an adhesive incorporating an antibacterial monomer DMAE-CB. *Journal of Biomedical Materials Research Part B: Applied Biomaterials* 2009;**90**:813–7.
67. Li F, Chen J, Chai Z, Zhang L, Xiao Y, Fang M, *et al*. Effects of a dental adhesive incorporating antibacterial monomer on the growth, adherence and membrane integrity of *Streptococcus mutans*. *Journal of Dentistry* 2009;**37**:289–96.
68. Chai Z, Li F, Fang M, Wang Y, Ma S, Xiao Y, *et al*. The bonding property and cytotoxicity of a dental adhesive incorporating a new antibacterial monomer. *Journal of Oral Rehabilitation* 2011;**38**:849–56.
69. Antonucci JM, Zeiger DN, Tang K, Lin-Gibson S, Fowler BO, Lin NJ. Synthesis and characterization of dimethacrylates containing quaternary ammonium functionalities for dental applications. *Dental Materials* 2012;**28**:219–28.
70. Li F, Weir MD, Chen J, Xu HHK. Comparison of quaternary ammonium-containing with nanosilver-containing adhesive in antibacterial properties and cytotoxicity. *Dental Materials* 2013;**29**:450–61.
71. Cheng L, Zhang K, Melo MAS, Weir MD, Zhou XD, Xu HHK. Anti-biofilm dentin primer with quaternary ammonium and silver nanoparticles. *Journal of Dental Research* 2012;**91**:598–604.
72. Zhang K, Cheng L, Imazato S, Antonucci JM, Lin NJ, Lin-Gibson S, *et al*. Effects of dual antibacterial agents MDPB and nano-silver in primer on microcosm biofilm, cytotoxicity and dentin bond properties. *Journal of Dentistry* 2013;**41**: 464–74.
73. Chen X, Schluesener HJ. Nanosilver: a nanoproduct in medical application. *Toxicology Letters* 2008;**176**:1–12.
74. Tolaymat TM, El Badawy AM, Genaidy A, Scheckel KG, Luxton TP, Suidan M. An evidence-based environmental perspective of manufactured silver nanoparticle in syntheses and applications: a systematic review and critical appraisal of peer-reviewed scientific papers. *Science of the Total Environment* 2010;**408**:999–1006.
75. Gunawan C, Teoh WY, Marquis CP, Amal R. Induced adaptation of *Bacillus* sp. to antimicrobial nanosilver. *Small* 2013;**9**:3554–60.
76. Braydich-Stolle L, Hussain S, Schlager JJ, Hofmann MC. In vitro cytotoxicity of nanoparticles in mammalian germline stem cells. *Toxicological Sciences* 2005;**88**:412–9.
77. Hsin YH, Chen CF, Huang S, Shih TS, Lai PS, Chueh PJ. The apoptotic effect of nanosilver is mediated by a ROS- and JNK-dependent mechanism involving the mitochondrial pathway in NIH3T3 cells. *Toxicology Letters* 2008;**179**:130–9.
78. Völker C, Oetken M, Oehlmann J. The biological effects and possible modes of action of nanosilver. *Review of Environmental Contamination and Toxicology* 2013;**223**:81–106.
79. Sahu SC, Zheng J, Graham L, Chen L, Ihrie J, Yourick JJ, *et al*. Comparative cytotoxicity of nanosilver in human liver HepG2 and colon Caco2 cells in culture. *Journal of Applied Toxicology* 2014. [Epub ahead of print].
80. Schäfer B, Brocke JV, Epp A, Götz M, Herzberg F, Kneuer C, *et al*. State of the art in human risk assessment of silver compounds in consumer products: a conference report on silver and nanosilver held at the BfR in 2012. *Archives of Toxicology* 2013;**87**:2249–62.

81. Kessler D, Theato P. Synthesis of functional inorganic-organic hybrid polymers based on poly(silsesquioxanes) and their thin film properties. *Macromolecules* 2008;**41**:5237–44.
82. Matyjaszewski K, Tsarevsky NV. Nanostructured functional materials prepared by atomic transfer radical polymerization. *Nature Chemistry* 2009;**1**:276–88.
83. Ghannam L, Parvole J, Laruelle G, François J, Billon L. Surface-initiated nitroxide-mediated polymerization: a tool for hybrid inorganic/organic nanocomposites in-situ synthesis. *Polymer International* 2006;**55**:1199–207.
84. Mandal H, Hay AS. Synthesis and characterization by MALDI-TOF MS of polycyclic siloxanes derived from p-substituted Novolac resins by MALDI-TOF MS. *Journal of Polymer Science A: Polymer Chemistry* 1998;**36**:2429–37.
85. Wallace WE, Guttman CM, Antonucci JM. Molecular structure of silsesquioxanes determined by matrix-assisted laser desorption/ionization time-of-flight mass spectrometry. *Journal of the American Society for Mass Spectrometry* 1999;**10**:224–30.
86. Grigoras S, Lane TH, Silicon-based polymer science: a comprehensive resource.Zeigler , Fearon G, editors. *Advances in Chemistry Series*, vol. 224. Washington, DC: American Chemistry Society; 1990. p. 125.
87. Mantellini MG, Botero TM, Yaman P, Dennison JB, Hanks CT, Nör JE. Adhesive resin induces apoptosis and cell-cycle arrest of pulp cells. *Journal of Dental Research* 2003;**82**:592–6.
88. El-kholany NR, Abielhassan MH, Elembaby AE, Maria OM. Apoptotic effect of different self-etch dental adhesives on odontoblasts in cell cultures. *Archives of Oral Biology* 2012;**57**:775–83.
89. Wyllie AH, Kerr JF, Currie AR. Cell death: the significance of apoptosis. *International Review of Cytology* 1980;**68**:251–306.